Colloids and Surfaces B: Biointerfaces 220 (2022) 112935

Contents lists available at ScienceDirect

Colloids and Surfaces B: Biointerfaces

journal homepage: www.elsevier.com/locate/colsurfb

Increased blood-brain barrier permeability of neuroprotective drug by colloidal serum albumin carriers

Viktória Hornok [a,*], Keristina Wagdi K. Amin [a,b], Alexandra N. Kovács [c], Ádám Juhász [a,c], Gábor Katona [d], György T. Balogh [e,f], Edit Csapó [a,c,**]

[a] Interdisciplinary Excellence Center, Department of Physical Chemistry and Materials Science, University of Szeged, H-6720 Rerrich B. sqr. 1, Szeged, Hungary
[b] Department of Chemistry, Suez Canal University, El Salam District, Ismailia 41522, Egypt
[c] MTA-SZTE Lendület "Momentum" Noble Metal Nanostructures Research Group, University of Szeged, H-6720 Rerrich B. sqr. 1, Szeged, Hungary
[d] Institute of Pharmaceutical Technology and Regulatory Affairs, Faculty of Pharmacy, University of Szeged, H-6720 Eötvös Str. 6, Szeged, Hungary
[e] Institute of Pharmacodynamics and Biopharmacy, Faculty of Pharmacy, University of Szeged, H-6720 Eötvös Str. 6, Szeged, Hungary
[f] Department of Chemical and Environmental Process Engineering, Budapest University of Technology and Economics, H-1111 Műegyetem Quay 3, Budapest, Hungary

ARTICLE INFO

Keywords:
Serum albumin
Kynurenic acid
Desolvation
Protein nanoparticles
Blood-brain barrier
Permeability

ABSTRACT

Encapsulation possibilities of two neuroprotective drugs of slightly different structures, kynurenic acid (KYNA) and its more hydrophilic analogue (SzR72), are studied in bovine serum albumin (BSA) nanoparticles (NPs) to increase their permeability through the blood-brain barrier (BBB). The effect of various preparation conditions such as protein concentration, protein-to-drug ratio, pH, ionic strength, type, and amount of desolvation agent and cross-linker concentration are discussed. It was found that the encapsulation proved to be successful only if the drugs are added to the pre-prepared BSA NPs. If the pH of the medium is adjusted to 4.0 instead of 7.4 the drug loading increased (from 4.5 % to 20.7 % for KYNA) due to the electrostatic interaction between the oppositely charged functional groups accompanied by significant secondary structural changes verified by circular dichroism spectroscopy (CD) suggesting the drug insertion in the hydrophobic pockets of BSA. The in vitro polar brain lipid extract (porcine) based permeability test proved the aimed three-, or fourfold higher BBB specific penetration for KYNA in the carrier relative to the unformatted drug.

1. Introduction

The encapsulation of drugs in colloidal particles for biomedical purposes is one of the most extensively investigated research area [1,2]. The application of such systems can be advantageous for several reasons, drug solubility can be increased, loss of drug activity can be eliminated, regulated release, or at least improved pharmacokinetics can be achieved thus reducing side effects relative to the conventional unformulated "free" drugs [3]. Several materials can be found in the literature functioning as drug carrying NPs or drug delivery systems (DDS) like synthetic and natural polymers (polysaccharides) [4], liposomes, micelles [5], dendrimers [6], *etc*. One of the most promising drug carriers are the serum albumins (SAs), due to their presence and abundance in the blood, they unquestionably manifest the requirements of potential formulation material [2,3,7]. The molecular structural arrangement of albumin involves a diversity of drug binding sites to the incorporation of water-soluble compounds and its relatively good affinity to encapsulate hydrophobic compounds, e.g. Ibuprofen, a non-steroidal anti-inflammatory drug (NSAID) is counted as stereotypical agents for binding to Sudlow's sites [8]. However, to promote drug delivery into the brain, novel, nanotechnology-based systems may offer future therapeutic options for several neurological disorders [9]. From the medical treatment point of view, migraine is considered one of the most disabling neurological conditions associated with high socio-economic costs. The application of the neuroprotective kynurenic acid (KYNA)-based therapy could be a solution for effective migraine treatment but due to its structure can hardly cross BBB, thus cannot be applicable directly for therapeutic purposes [10]. Hence our study aims to investigates the KYNA and one of its analogs for increasing therapeutic efficiency. The formula discussed in our former manuscript [11] resulted in a US patent

* Corresponding author.
** Corresponding author at: Interdisciplinary Excellence Center, Department of Physical Chemistry and Materials Science, University of Szeged, H-6720 Rerrich B. sqr. 1, Szeged, Hungary.
E-mail addresses: vhornok@chem.u-szeged.hu (V. Hornok), juhaszne.csapo.edit@med.u-szeged.hu (E. Csapó).

https://doi.org/10.1016/j.colsurfb.2022.112935
Received 2 August 2022; Received in revised form 2 September 2022; Accepted 13 October 2022
Available online 14 October 2022
0927-7765/© 2022 The Author(s). Published by Elsevier B.V. This is an open access article under the CC BY license (http://creativecommons.org/licenses/by/4.0/).

(US10857236B2) encapsulating KYNA in core-shell type BSA NPs using polyallylamine hydrochloride as the shell material [11]. The application of protein-based delivery system resulted in a two-fold drug permeability through the BBB. There are few other studies relating to the encapsulation of KYNA in SAs, but there is not one for desolvated BSA. Among the preparation methods applied for the SAs, desolvation is a reproducible and robust method [8]. Depending on the applied drug molecule, however, the preparation conditions must be modified accordingly to reach required NP properties such as hydrodynamic diameter, surface charge and functional groups, *etc* [12]. In general, the desolvation method offers several advanced modifications of the albumin's tertiary structure which will lead to nano-sized particles and more hydrophobic sites providing an ideal approach for the production of protein-based NPs with controlled properties [13]. If the amount of encapsulated drug molecule per carrier is high, the drug potency is higher deliver therapeutically relevant amounts of that certain drug thus we aim to investigate the effect of various preparation conditions on the properties of the forming BSA NPs by also determining the drug-loading (DL %), encapsulation efficiency (EE %), release and BBB-specific permeability for drugs of neuroprotective activity, along with changes in the protein structure caused by the encapsulation.

2. Materials and methods

2.1. Materials

Kynurenic acid ($\geq$ 98 %), sodium dihydrogen phosphate monohydrate ($NaH_2PO_4 \times H_2O$, $\geq$ 99 %), disodium-hydrogen phosphate (Na_2HPO_4, $\geq$ 99 %), potassium dihydrogen phosphate dihydrate ($KH_2PO_4 \times 2\,H_2O$, $\geq$ 99 %), glutaraldehyde solution (GA, $\geq$ 98.0 %) and BSA (lyophilized powder, $\geq$ 98.0 %), brain polar lipid extract and cholesterol were all purchased from Sigma-Aldrich (Budapest, Hungary), with analytical purity and were used as received. Sodium chloride (NaCl, $\geq$ 98 %), sodium acetate (CH_3COOH, $\geq$ 98 %), acetic acid (CH_3COOH, $\geq$ 99 %) was acquired from Molar Ltd (Budapest, Hungary). The KYNA analogue, SzR72 was provided by the Institute of Pharmaceutical Chemistry of the University of Szeged (Scheme S1) [14]. The solvents like methanol, ethanol, acetone and acetonitrile were used without further purification. Ultrapure water was produced by deionization and filtration with a Millipore purification apparatus (18.2 MΩ·cm at 25 °C).

2.2. Methods

2.2.1. Preparation of BSA, BSA/KYNA and BSA/SzR72 NPs

As Scheme S2 shows, the BSA NPs were prepared by dissolving 2 mL of 10–100 mg/mL BSA solution then addition (1 mL/min) of the of desolvating agent, e.g. 5 mL of ethanol, acetone, acetonitrile or methanol under constant stirring (500 rpm) till the solution became turbid. After 30 min, 0–30 μL of 8 % of GA solution was added to induce particle cross-linking and stirred for at least 18 h at room temperature. Then the NPs were purified by repeated centrifugation (30 min at 14 000 rpm) and washing steps to remove non-desolvated BSA, GA and organic solvents. After the supernatant was removed, the NPs were redispersed in 2 mL of MQ water and centrifugated again. The final material was redispersed in 3 mL buffer solution, either in phosphate buffer saline solution (PBS) at pH = 7.4 or in acetate buffer solution at pH = 4.0. Different amounts of molecules ($n_{drug\ /\ BSA}$ = 0–35) was added to the purified BSA NPs at both pH then the mixture was stirred for hours. The samples were purified through the same way as the drug-free NPs and were freeze-dried using Christ Alpha 1–2 LD plus.

2.3. Instrumental

2.3.1. Light scattering

The average particle size (d_{ave}), polydispersity index (PDI) and ζ-potential of the NPs were determined by Horiba SZ-100 Nanoparticle Analyzer (Retsch Technology GmbH, Germany) The ζ-potential measurements were performed in a carbon-electrode type cell. Dispersed samples were diluted in the appropriate aqueous buffer solution and the measurements were performed at a scattering angle of 90° at 25 °C ± 0.2 °C. The average diameters and standard deviations (SD) of five measurements are calculated.

2.3.2. Microscopy

The transmission electron microscopy (TEM) images were registered by using a Jeol JEM-1400plus equipment (Japan) at 120 keV accelerating voltage and were analyzed by ImageJ software to study the particle size, the shape and the morphological behaviours of the prepared BSA NPs and drug-loaded BSA NPs. Dissolved NPs were diluted 10 times with MQ water one drop from the solutions were dropped on a Formvar-foil covered copper grid and samples were left for complete drying. Then, dried NPs on the grids were used for TEM analysis.

2.3.3. Spectroscopy

The infrared spectra (IR) of the freeze-dried samples were recorded by Jasco FT/IR-4700 equipment in an attenuated total reflectance (ATR) mode. The spectra were registered at room temperature by accumulating 128 interferogram at 1 cm^{-1} resolution.

Circular Dichroism (CD) spectra of both dispersed samples and powder samples were measured by using Jasco J-1100 CD spectrometer (ABL & JASCO, Hungary) at 25 ± 0.5 °C using 1 cm optical path length quartz cuvette with a was a water-cooled, high-energy xenon lamp (450 W) light source. All the spectra were registered in the middle UV-region (200−300 nm) at 100 nm/min scanning speed under N_2 flow (3 L/min) and the final spectra represents the mean of 3 scans. The curves were corrected with the background spectrum (buffer or drug-containing buffer solution) using the Spectra Manager™ software.

2.3.4. Determination of encapsulation properties

The amount of encapsulated drug in the NPs was determined indirectly from the UV-spectra, as follows. Supernatants were collected and used to calculate the percentage of the non-encapsulated drug by measuring the absorbance of the MQ diluted solution at 332 nm and 338 nm for KYNA and SzR72 respectively, using a UV–1800 (Shimadzu) double beam spectrophotometer. The absorbance value was using a standard calibration curve prepared with known concentrations of KYNA/SzR72 in MQ water and also in buffer. The encapsulation efficiency (EE %) and the drug loading percentage (DL %) was calculated using equations presented previously in our article [15].

2.3.5. In vitro drug release and permeability studies

The in vitro release of the molecules from the lyophilized drug-loaded NPs was carried out by detecting the characteristic absorbance band of drug at certain wavelength, e.g. 332 nm for KYNA transferred through a cellulose semi-permeable membrane having M_w Cut-Off (MWCOs) of 14,000 (Sigma-Aldrich). The release experiments were carried out in PBS (37.5 °C) at pH = 7.4 under continuous stirring both with the drug itself without the BSA carrier [16]. The obtained amount expressed in release percentage was plotted against time. Several mathematical models were used to evaluate the release kinetics and mechanism based on our previously published routine [15]. Parallel artificial membrane permeability assay (PAMPA) was used to determine the effective BBB permeability of BSA-based formulas in comparison to initial KYNA reference solution. The detailed description of the PAMPA measurements was summarized in Supplementary.

3. Results and discussion

3.1. Preparation of pure BSA NPs

3.1.1. Effect of desolvating agent on NPs formation

The effect of amount and type of desolvating agents such as methanol, ethanol, acetone was investigated on the properties of forming NPs, like size distribution and relative yield. The BSA solution of 30 mg/mL turned turbid upon the addition of 1:6 (V/V) of methanol, 1:2.5 (V/V) of ethanol, acetone and acetonitrile. The turbidity for the methanol-containing system is significantly less even observing by naked eye (Fig. 1) indicating the difference in the amount of forming NPs. To characterize the above-mentioned particle – to initial protein concentration (turbidity relation) the yield for the NP formation was determined by determining the solid content in the dispersion. Addition of the desolvating agent to an aqueous solution of BSA produced considerable amount of BSA NPs with 25.5 ± 3.5 %, 23.6 ± 1.6 %, 21 ± 1.1 %, and 1 ± 0.2 % yields of NPs, respectively (Fig. 1B). These results indicate that alcohols with short carbon chains have poor desolvation ability for BSA. On the other hand, the hydrodynamic sizes, PDI and ζ-potential of BSA NPs using different desolvating agents were measured. Their average sizes varied between ~100 and 170 nm, whilst the ζ-potentials of the produced NPs were found to be between − 55 and − 39 mV. The exception was only observed in the case of methanol since a lower net negative potential of −25 mV was obtained. If one compares the TEM images of different desolvating agent-containing samples, the methanol-containing is strikingly different (Fig. S1). Besides the type of desolvating agent, the amount necessary to achieve best yield and monodispersity was also examined in this study. The step-by-step addition of EtOH was followed by determining NTU values of the dispersion by turbidimeter, thus determining the minimum to optimal amount of reagent for particle formation. The addition of desolvating agent on turbidity shows a S-shape curve as it can be seen in Fig. 1A. It was observed that $V_{EtOH}/V_{water} = 2.5$ is sufficient for the optimum preparation of BSA NPs. NPs can form below, just with less yield. Moreover, it has also an effect on the separation ability during the purification process. Purification was not available up to addition of 1.5-fold volume of EtOH is reached because the low amount was not sufficient to induce NP formation. Above 2-fold volume, it became more and more turbid at ratio of 2.5 indicating higher yield. But continuing the addition of ethanol decrease the turbidity of the solution without affecting the size of NPs.

3.1.2. Effect of protein concentration

There is a contradiction in the literature about the effect of BSA concentration on the particles size by the existence of several parameters that can affect nanoparticle size for each study. First, we aimed to study the effect of initial protein concentration on properties of forming NPs, to determine the suitable concentration range of BSA for preparation of NPs with high stability and favourable sizes (namely the average diameter, polydispersity and ζ-potential with appropriate SD values). The results can be seen in Fig. 2. and Table 1. The average diameter gradually increases from 97.90 nm to 168.47 nm as the c_{BSA} changes from 10 mg/mL to 100 mg/mL (Fig. 2A), respectively. The PDI decreases accordingly, while dosen't show significant change over 30 mg/mL BSA content. The concentration of BSA influences the particle production process by the rate of nucleation and aggregation explained by the nucleation theory. As the frequency of albumin transport between the ethanol and water is lowered the nucleation rate decreases resulting in particles with larger size. Oppositely, high protein concentration leads to higher extent of supersaturation. Therefore, smaller nuclei are produced but the high degree of supersaturation accelerates the aggregation and NPs with larger d_{AV} are produced as the possibility of particle collision is higher. The TEM images indicate NPs of spherical morphology with similar average particle diameter (120 nm for sample 60 mg/mL, Fig. 2B). The BSA concentrations higher than this value did not produce particles smaller than 160 nm. The ζ-potential values of the produced NPs refer to colloidally stable dispersion in the range of − 34.1 to − 40.5 mV. The negative value is due to the terminal groups of BSA of negative charges are positioned on the surfaces of the NPs.

3.1.3. Effect of cross-linker amount

GA can stabilize and bind many BSA molecules in the particle matrix through the amino moieties in lysine residues. The degree of cross-linking and therefore the degree of free amino groups are important factors through their impact on the biodegradability of the particles. Additionally, free amino groups can be used to link drugs or other active ingredients to the NP surface. Some studies found that at least 0.2 μL (8 % GA)/mg BSA is needed for stabilization and obtaining favourable sizes, but other studies use higher amount. Excess of GA led to the redissolvation of 30 % of HSA NPs upon dilution with water, thus the particles were not sufficiently stabilized by cross-linking [17]. In our case the BSA particles was treated with different amounts 0–30 μL of 8 % GA (from 0.0 μL (8 % GA)/mg BSA to 1.0 μL (8 % GA)/mg BSA) to determine the effect of different volumes of GA on the size of NPs (Fig. 2C). We obtained that the concentration of GA had little effect on PDI or particle size (d ~ 120 nm) above a minimum value of about 10 μL

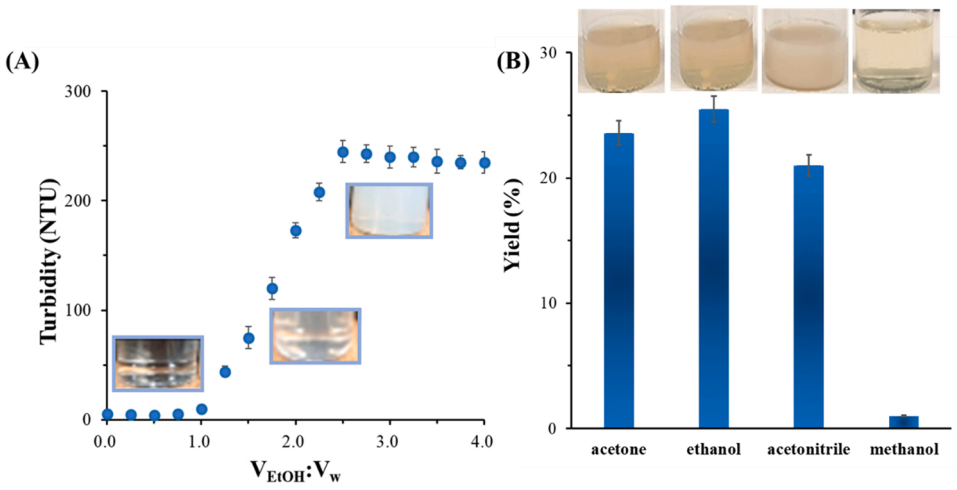

Fig. 1. Turbidity of BSA solution in relation to the ethanol addition (A) and yield (%) of BSA NPs using different desolvating agents (B). The appropriate photos taken of the dispersions can be seen.

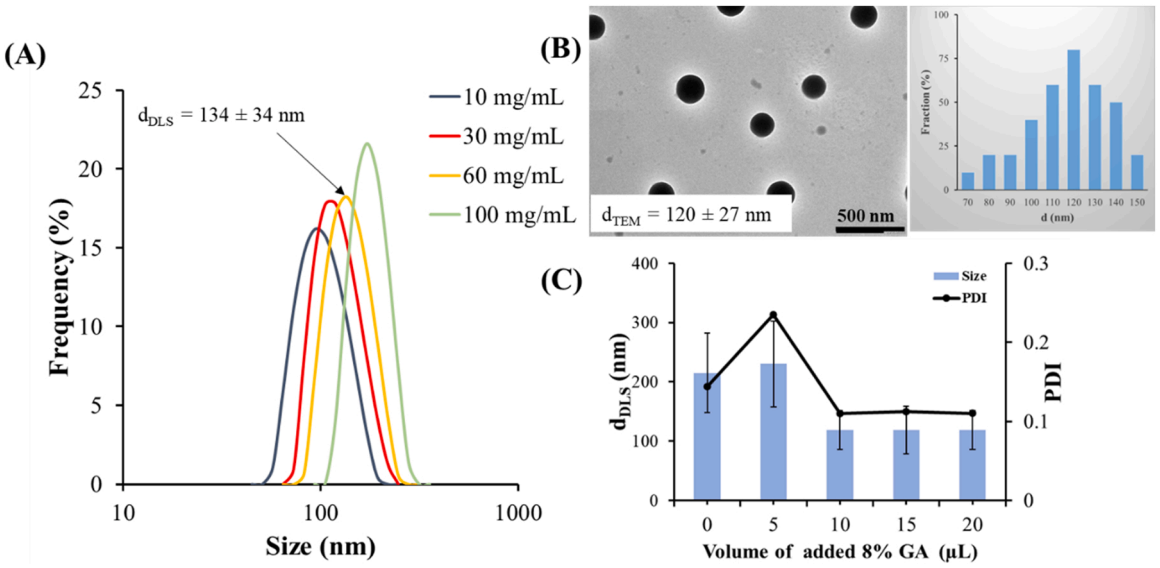

Fig. 2. Particle size distribution of the NPs produced from BSA solutions of different initial protein concentration determined from DLS (A), and TEM image with the size distribution of sample using c_{BSA} = 60 mg/mL (B). Change of the particle size and the PDI as a function of the used GA cross-linker (c_{BSA} = 30 mg/mL) (C).

Table 1
Characteristics of BSA NPs prepared at different initial BSA concentration: average hydrodynamic diameter (DLS), polydispersity index (PDI) and ζ -potential with the appropriate SD values.

c_{BSA} mg/mL	d_{ave} (nm)			PDI			ζ-potential (mV)		
10	98	±	26	0.134	±	0.002	-34.1	±	0.115
20	109	±	27	0.124	±	0.001	-34.3	±	0.300
30	119	±	33	0.110	±	0.001	-40.5	±	0.058
60	134	±	32	0.112	±	0.004	-40.3	±	0.252
100	168	±	34	0.112	±	0.002	-34.1	±	0.058

(0.33 µL GA/ mg BSA).

3.2. Drug encapsulation and structural changes

3.2.1. Encapsulation of KYNA

Although water solubility of KYNA is low (50 mg/mL in 1 M NaOH solution) but dispersion of BSA NPs in phosphate buffer (at pH = 7.40), enhanced its solubility. At 35:1 (KYNA: BSA) molar ratio (the theoretical amount of added drug to the actual amount of BSA NPs, as determined in 3.1.1.), samples started to aggregate. This slight increase in particle size indicates the successful encapsulation of KYNA (Fig. 3A). The particle size measurements from TEM analysis were comparable with those of DLS, indicating that the particle diameters varied between 100 ± 30 nm to 132 ± 40 when the experiments were carried out at pH = 7.40. At lower pH slightly larger NPs are formed, the PDI of KYNA-loaded BSA NPs indicates a monodisperse system, with values ranging from 0.13 to 0.33. The amount of encapsulated KYNA was indirectly determined spectrophotometrically from the supernatant, using a calibration curve. The DL % and EE % of KYNA into BSA NPs at pH = 7.40 (Fig. 3B) and pH = 4.00 (Fig. 3C) are also shown in Fig. 3. At low n_{KYNA}:n_{BSA} molar ratio the EE % as well as the DL is low. Increase in the n_{KYNA}:n_{BSA} molar ratio both show higher values, but reach maximum at a given point (pH = 7.40, n_{KYNA}:n_{BSA} 25:1, EE % = 14.0 %, DL % = 4.53 %. (pH = 4.00, n_{KYNA}:n_{BSA} 25:1, EE % = 72.4 %, DL % = 20.8 %). It was obtained that at acidic conditions measurable higher (approx. 4-fold) amount of KYNA can be encapsulated which confirm the slightly higher size of NPs at pH = 4.0. Above 100:1 n_{KYNA}:n_{BSA} molar ratio, the EE % starts to decrease but the DL % was almost the same indicating that the carrier can't load more of the drug. The observed low EE % may be attributed to the low affinity of BSA to KYNA as a hydrophobic molecule. For this reason, the next drug we chose to encapsulate was the hydrophilic kynurenate analogue SzR72.

3.2.2. Encapsulation of SzR72 molecule

In case of SZR72, NPs with mean diameter of 121–145 nm were produced. The PDI of SzR72-loaded BSA NPs revealed a relatively monodisperse system, with PDI values ranging from 0.12 to 0.30. The highest PDI value and the largest particle average size was observed at 35:1 n_{SzR72}:n_{BSA} molar ratio where we achieved the highest EE % (23 %, Fig. 3D). The ζ-potential of the SzR72-loaded samples did not differ so much from that of the free BSA NPs, it was − 38.21 mV at the highest EE %. This slight decrease in negativity clarified that the presence of SzR72 resulted in having BSA NPs with a bit more cationic surface charge. The EE % increases as the n_{SzR72}:n_{BSA} increases. Above 137:1 molar ratio where the EE % is the highest (23 %) the carrier can't load more of the kynurenic acid analogue (with 14.7 wt. % drug contain). As expected, the observed EE % of SzR72 into BSA was higher than that of KYNA partly due to the higher affinity of BSA to SzR72 as a hydrophilic molecule and also because of the higher number of nitrogen atoms in SzR72 with the possibility to form more hydrogen bond [18]. The determined EE % and DL % at physiological condition pH = 7.4, resulted in negatively charged albumin surface. Isoelectric point (IEP) of BSA is 4.5–5.0; albumin exists in a relatively neutral, zwitterion form. The amount of encapsulated drug can be enhanced by ensuring attraction between the drug and the carrier [19]. For KYNA drug, pH = 4.0 was chosen to enable the encapsulation of increased amount to ensure oppositely charged functional groups of the two components, as the pK_a of KYNA is ~ 4.5 (Fig. 3D).

3.2.3. Structural characterization by FT-IR and CD spectroscopy

To gain information how the encapsulated drug effects the structure of the protein, FT-IR spectrum analysis was carried out. It was possible to observe the major bands of pure BSA at 1640 cm^{-1} (amide I, C═O stretching), 1514 cm^{-1} (amide II, related to C–N stretching and N–H bending vibrations) and 1394 cm^{-1} (CH_2 bending groups). The most intense bands are associated with the secondary structure and conformation of proteins [20]. The spectra of KYNA–BSA NPs and (SZR72)–BSA NPs exhibited these characteristic bands of the protein as well as the characteristic vibrations of C-N, C-O(H) and CH bends which are related to the structure of KYNA and SZR72 (Fig. S2). A small shift of the absorption bands was observed when compared to pure BSA with BSA NPs

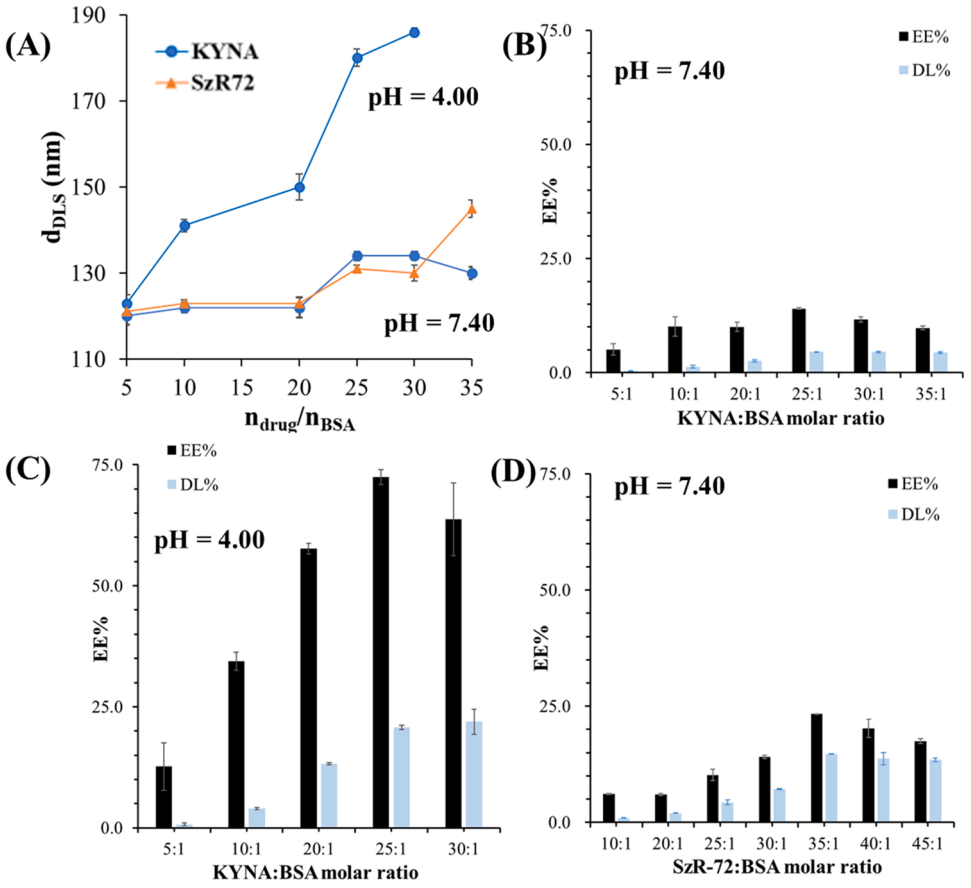

Fig. 3. Average hydrodynamic diameter of drug-loaded NPs in relation to the n_{drug}:n_{BSA} ratio at different pH (A). Encapsulation efficiency (EE %) and drug loading (DL %) percentage of BSA/KYNA NPs (pH = 7.4) (B), BSA/KYNA NPs (pH = 4.0) (C), and BSA/SzR72 NPs (pH = 7.4) (D).

and drug loaded BSA NPs. The related changes in the amide I and II bands confirm the formation of albumin NPs and drug loaded NPs. Besides FT-IR CD spectroscopy is also suitable to follow the structural changes of proteins. The distinctive feature for α-helical structure attributed to the n-π * and π-π * transitions of the peptide bond carbonyl group two strong negative absorption bands close to 208 and 222 nm [21]. The registered CD spectra at different pH (Fig. 4) indicate that the change of the pH somewhat alters the structure of serum protein; ~ 10 % difference can be detected for pure BSA and for BSA NPs. On the other hand, we can obtain that the desolvation method does not distort significantly the BSA structure, in the proportion of the secondary structural elements. The conformation of the protein as an effect of KYNA and SZR72 addition provides information about the possibility of BSA-KYNA/SZR72 interaction. The proportions of the secondary structural elements for both systems at pH = 7.4 and pH = 4.0 were evaluated using Reed model [22]. Addition of the drug molecules to the BSA NPs causes the decrease of α-helix content. Namely, the model estimates the α-helix content of the drug-free BSA NPs to 28.7 % which is in good agreement with the values determined with different methods elsewhere [23]. After the addition of KYNA and SZR72, the value is decreased to 25.0 % and 19.3 % for the benefit of β-sheet and random conformation contents, respectively (Table 2). The most dominant shift is detected for

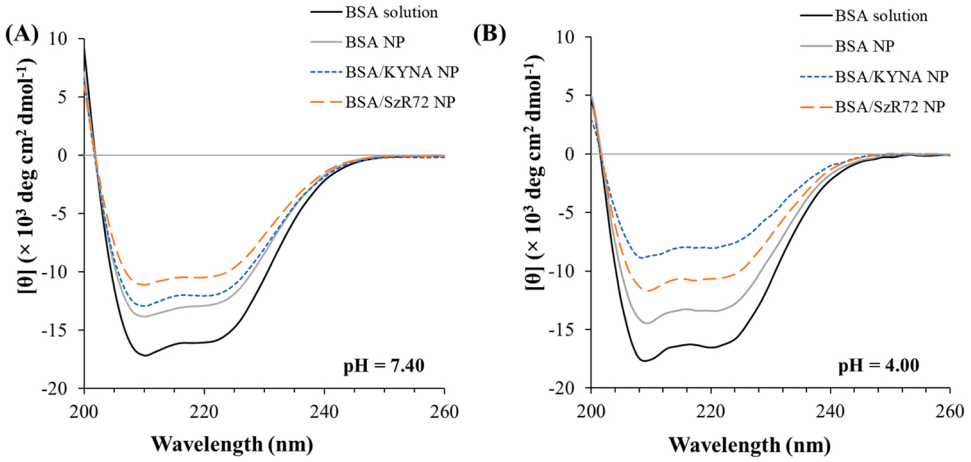

Fig. 4. CD spectra of the BSA solution, the drug-free BSA NPs and drug-containing dispersions and at pH = 7.4 (A) and pH = 4.0 (B). (c_{BSA} = 30 μg/mL, T = 25 °C).

Table 2
Percentage of the secondary structural elements of BSA solution, the drug-free dispersions and the drug-containing determined by Reed model-fitted results and calculations from the CD spectra at different pH.

secondary structural elements		solution			dispersions					
		BSA			BSA		BSA/KYNA		BSA/SZR72	
		pH7.4	pH4.0		pH7.4	pH4.0	pH7.4	pH4.0	pH7.4	pH4.0
Reed model-fitted	α-Helix (%)	39.1	41.6		28.7	30.1	25.0	12.2	19.3	20.6
	β-sheet (%)	44.2	39.0		46.7	45.4	48.9	50.5	51.1	49.3
	Turn (%)	0.0	0.0		0.9	0.0	0.0	2.2	0.9	0.5
	Random (%)	16.7	19.4		23.7	24.5	26.1	35.1	28.8	29.6
	RMS*	7.26	6.40		7.59	6.89	8.41	9.42	8.78	7.97
calculated	α-Helix (%)	42.7		46.3	32.2	34.8	29.1	16.7	23.1	25.2

*RMS = Root Mean Square.

pH = 4.0 for BSA/KYNA system (α-helix from 30.1 % to 12.2 %), which is in good agreement with our experience that at acidic pH the BSA NPs encapsulate more KYNA. The values of α-helix contents are also verified by the calculated amounts presented in Table 2. The calculated values (equations of Eq. 1 and Eq. 2 from Ref [21]) are consistent with those calculated from fitting the spectra with the Reed model in both pH suggesting the presence of drugs in the protein structure [24].

3.2.4. Drug release

In vitro drug release studies of the unformatted drugs and drugs loaded into BSA particles were carried out by using semipermeable membrane where the drugs were detected spectrophotometrically. The encapsulated drug in the inner core of the BSA NPs diffuses slowly from the carrier to the release medium compared to diffusion of the free molecules without carrier. For KYNA-loaded BSA (Fig. S3A), an initial burst of KYNA release within the first 100 min, during which up to 40.0 % of the loaded drug is released from BSA NPs. The total release of KYNA was found to be 45 % in the examined time, while nearly 100 % of the free molecules pass through the membrane. In case of SzR-72-loaded BSA (Fig. S3B), 40 % of loaded drug is released from NPs after 120 min. The total release was found to be almost 47 % in the examined time interval, while only ~ 71 % can be detected for pure SZR-72. These observations are in agree with many studies in which BSA NPs has been applied as nanocarrier [3,11]. The dissolution curves were fitted by different kinetic models to provide information on drug release mechanism. To define that what is the best mathematical model of each release data series, the nonlinear chi-square (χ^2) error analysis method was used [25]. Nonlinear chi-square test is a necessary statistical tool for the nonlinear regression, obtained by determining the sum squares differences between the experimental and the calculated data, with each squared difference divided by its comparable value (calculated from the models). When the data from model are nearly same as the experimental data, χ^2 will be a small number and if they are strongly different, χ^2 will be a bigger value. Based on an earlier presented study [26] six different and well-known release equation was tested to describe the change of experimental data as a function of time. The release data were fitted by rate equations with an analytical solution (First- and Second Order Rate equations), empirical formulas (Weibull and Korsmeyer–Peppas) and Higuchi equation what was developed to describe the drug release as a diffusion process based on Fick's law. The calculated values of χ^2 for the dissolution of free drugs as well as the drugs encapsulated into BSA NPs are summarized in Fig. S4. Based on the χ^2 error analysis method we found that, in the case of KYNA the Weibull equation while in the case of SZR72 the Second Order rate equation was able to describe the experimental results most accurately. As can be seen on the Fig. S4. in the case of both drugs, the encapsulation significantly changed the way of dissolution. In the case of protein-encapsulated KYNA, second-order kinetics is the most adequate, while for SZR72, Weibull empirical correlation can correctly describe the release process. These data clearly confirm that the combination of BSA and KYNA or SZR72 can strongly prolong drug release at pH = 7.4 (in PBS) while the KYNA/BSA composite can moderate the rate of the dissolution in a gentler way.

3.2.5. Blood-brain barrier permeability study

The results about BBB-PAMPA permeability test of KYNA-containing formulations prepared them at pH = 7.40 and at pH = 4.0 are shown in Fig. 5. The permeability studies have been performed only for the KYNA-containing composite, because, as shown in Fig. 3, higher DL % can be achieved with this drug at pH = 4.0. Both NP formulation showed elevated Flux (Fig. 5), BBB-specific permeability (Pe) and membrane retention (MR) referred to pure KYNA (Table 3). Based on the Pe/MR data summarized in Table 3, it can be assumed that the three- to four-fold increase in permeability of KYNA in the case of BSA formulations can be attributed to increased membrane retention. That is, the BSA-based NP greatly facilitated the interaction between KYNA and the BBB-specific lipid, which is a mechanistically critical step for drug permeability. In accordance with this finding, the BBB-specific flux values of KYNA (Fig. 5.) also showed significantly higher values for the two BSA-based formulations compared to the unformulated KYNA (BSA/KYNA (pH = 7.4) vs. KYNA * ** , $p < 0.001$; BSA/KYNA (pH = 4.0) vs. KYNA * ** , $p < 0.001$). The increased flux of BSA NPs can be explained by as a result of two effects. In addition to the permeability, the equilibrium solubility of KYNA in the NP formulations also increased significantly compared to the pure KYNA due to solubilizing effect of

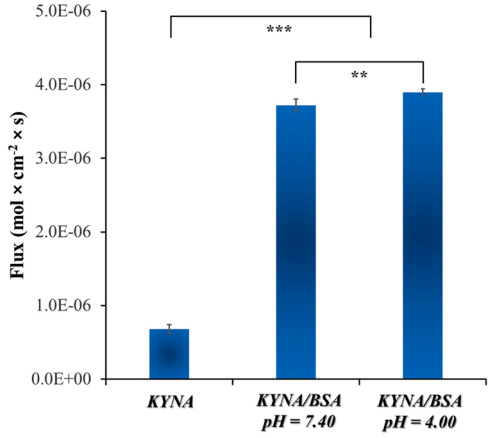

Fig. 5. Flux values of BBB-PAMPA permeability study of BSA/KYNA NPs compared to initial KYNA calculated by Eq.S3. Statistical analysis: *t*-test. * * $p < 0.01$, * ** $p < 0.001$ compared to initial KYNA control or formula.

Table 3
Blood-brain barrier (BBB) PAMPA permeability (P_e) and membrane retention (MR) values.

	Pe ($\times 10^{-7}$ cm $\times$ s^{-1})		MR (%)	
	Mean	SD	Mean	SD
KYNA	4.0	0.35	-0.3	0.8
KYNA/BSA (pH = 7.40)	16.3	0.37	16.1	0.7
KYNA/BSA (pH = 4.00)	12.8	0.16	14.0	1.2

BSA. Comparing the flux of BSA/KYNA NPs prepared at pH = 7.4 to the NPs at pH = 4, significant difference was observed (pH = 7.4 vs. pH = 4.0 **, $p < 0.01$), which can be explained by the increased solubilizing effect of the BSA nanoparticle system as the chosen pH for the preparation due to the possibility of electrostatic attraction between the oppositely charges species, ensures higher drug content and stronger interaction in the formula.

4. Conclusions

Synthesis parameters affecting the potential biomedical application of neuroactive KYNA-, and SzR72-containing desolvated BSA NPs were studied in this work. The optimal initial concentration of the protein is determined to be 30 mg/mL with ethanol as the desolvating agent. The $V_{ethanol}$:V_{water} volume ratio should be kept above 2.5 to achieve stable NPs confirmed from turbidity detection. Under these conditions, the nucleus formation speed determines the average particle size of the NPs, thus monodisperse, stable BSA NPs formed, with an average hydrodynamic diameter of 118 ± 32 nm that can be taken up by entrances of endothelial cells. For successful encapsulation, contrary to other drugs, both KYNA and SzR72 should be added to the pre-produced BSA NPs. The maximum achieved DL % for KYNA and SzR72 was 20.5 % and 14.7 %, respectively at pH = 7.4. To further increase the efficiency, pH = 4 was chosen, hereby significantly higher EE %, namely 76 %, was achieved for the KYNA molecule moreover, by the careful adjusting of synthesis parameters, more monodisperse system can be formed with less distorted protein structure. If we compare our results with our previous one presented in the patent, we can state that the desolvated BSA NPs achieved higher three-, or four-fold BBB permeability relative to the unformulated drug, facilitating both KYNA retention and flux by increasing its solubility.

CRediT authorship contribution statement

Viktória Hornok: Conceptualization, Writing – original draft, Writing – review & editing, **Keristina Wagdi Kamil Amin:** Methodology, Investigation, Visualization, **Alexandra N. Kovács**: Methodology, Investigation, **Gábor Katona:** Methodology, Investigation, **Ádám Juhász**: Validation, Formal analysis, Visualization, **György T. Balogh:** Methodology, Investigation, **Edit Csapó**: Conceptualization, Visualization, Writing – original draft, Writing – review & editing, Supervision, Resources.

Declaration of Competing Interest

The authors declare that they have no known competing financial interests or personal relationships that could have appeared to influence the work reported in this paper.

Data availability

Data will be made available on request.

Acknowledgements

The research was supported by the National Research, Development and Innovation Office (NRDIH) through the project FK131446. Project no. TKP2021-EGA-32 has been implemented with the support provided by the Ministry of Innovation and Technology (MIT) of Hungary from the National Research, Development and Innovation Fund (NRDIF), financed under the TKP2021-EGA funding scheme. K.W.K.A. is funded by a scholarship under the joint executive program between the Arab Republic of Egypt and Hungary. This work was also supported by the ÚNKP-22–5-SZTE-569 and ÚNKP-22-4-SZTE-497 New National Excellence Program of the MIT from the source of the NRDIF. This paper was supported by the János Bolyai Research Scholarship of the Hungarian Academy of Sciences (V.H.).

Appendix A. Supporting information

Supplementary data associated with this article can be found in the online version at doi:10.1016/j.colsurfb.2022.112935.

References

[1] N. Larson, H. Ghandehari, Polymeric conjugates for drug delivery, Chem. Mater. 24 (2012) 840–853, https://doi.org/10.1021/cm2031569.
[2] A. Jain, S.K. Singh, S.K. Arya, S.C. Kundu, S. Kapoor, Protein nanoparticles: promising platforms for drug delivery applications, ACS Biomater. Sci. Eng. 4 (2018) 3939–3961, https://doi.org/10.1021/acsbiomaterials.8b01098.
[3] P. Singh, H. Singh, V. Castro-Aceituno, S. Ahn, Y.J. Kim, D.C. Yang, Bovine serum albumin as a nanocarrier for the efficient delivery of ginsenoside compound K: preparation, physicochemical characterizations and in vitro biological studies, RSC Adv. 7 (2017) 15397–15407, https://doi.org/10.1039/c6ra25264h.
[4] E. Csapó, H. Szokolai, Á. Juhász, N. Varga, L. Janovák, I. Dékány, Cross-linked and hydrophobized hyaluronic acid-based controlled drug release systems, Carbohydr. Polym. 195 (2018) 99–106, https://doi.org/10.1016/j.carbpol.2018.04.073.
[5] D. Guimarães, A. Cavaco-Paulo, E. Nogueira, Design of liposomes as drug delivery system for therapeutic applications, Int. J. Pharm. 601 (2021), 120571, https://doi.org/10.1016/j.ijpharm.2021.120571.
[6] Y. Zhu, C. Liu, Z. Pang, Dendrimer-based drug delivery systems for brain targeting, Biomolecules 9 (2019) 790, https://doi.org/10.3390/biom9120790.
[7] F.F. An, X.H. Zhang, Strategies for preparing albumin-based nanoparticles for multifunctional bioimaging and drug delivery, Theranostics 7 (2017) 3667–3689, https://doi.org/10.7150/thno.19365.
[8] A. Jahanban-Esfahlan, S. Dastmalchi, S. Davaran, A simple improved desolvation method for the rapid preparation of albumin nanoparticles, Int. J. Biol. Macromol. 91 (2016) 703–709, https://doi.org/10.1016/j.ijbiomac.2016.05.032.
[9] F. Kratz, A clinical update of using albumin as a drug vehicle — a commentary, J. Control. Release 190 (2014) 331–336, https://doi.org/10.1016/J.JCONREL.2014.03.013.
[10] L. Vécsei, M. Lukács, J. Tajti, F. Fülöp, J. Toldi, L. Edvinsson, The therapeutic impact of new migraine discoveries, Curr. Med. Chem. 26 (2018) 6261–6281, https://doi.org/10.2174/0929867325666180530114534.
[11] N. Varga, E. Csapó, Z. Majláth, I. Ilisz, I.A. Krizbai, I. Wilhelm, L. Knapp, J. Toldi, L. Vécsei, I. Dékány, Targeting of the kynurenic acid across the blood-brain barrier by core-shell nanoparticles, Eur. J. Pharm. Sci. 86 (2016) 67–74, https://doi.org/10.1016/j.ejps.2016.02.012.
[12] K. Langer, S. Balthasar, V. Vogel, N. Dinauer, H. Von Briesen, D. Schubert, Optimization of the preparation process for human serum albumin (HSA) nanoparticles, Int. J. Pharm. 257 (2003) 169–180, https://doi.org/10.1016/S0378-5173(03)00134-0.
[13] A.O. Elzoghby, W.M. Samy, N.A. Elgindy, Albumin-based nanoparticles as potential controlled release drug delivery systems, J. Control. Release 157 (2012) 168–182, https://doi.org/10.1016/j.jconrel.2011.07.031.
[14] K. Nagy, I. Plangár, B. Tuka, L. Gellért, D. Varga, I. Demeter, T. Farkas, Z. Kis, M. Marosi, D. Zádori, P. Klivényi, F. Fülöp, I. Szatmári, L. Vécsei, J. Toldi, Synthesis and biological effects of some kynurenic acid analogs, Bioorg. Med. Chem. 19 (2011) 7590–7596, https://doi.org/10.1016/j.bmc.2011.10.029.
[15] N. Varga, Á. Turcsányi, V. Hornok, E. Csapó, Vitamin e-loaded pla- and plga-based core-shell nanoparticles: synthesis, structure optimization and controlled drug release, Pharmaceutics 11 (2019) 357, https://doi.org/10.3390/pharmaceutics11070357.
[16] A. Avdeef, Absorption and drug development: solubility, permeability, and charge state, Absorpt. Drug Dev. Solubility, Permeab., Charg. State (2012), https://doi.org/10.1002/9781118286067.
[17] C. Weber, C. Coester, J. Kreuter, K. Langer, Desolvation process and surface characterisation of protein nanoparticles, Int. J. Pharm. 194 (2000) 91–102, https://doi.org/10.1016/S0378-5173(99)00370-1.
[18] R.C. Pedrozo, E. Antônio, N.M. Khalil, R.M. Mainardes, Bovine serum albumin–based nanoparticles containing the flavonoid rutin produced by nano spray drying, Braz. J. Pharm. Sci. 56 (2020) 17692, https://doi.org/10.1590/s2175-97902019000317692.
[19] S.C. Sozer, T.O. Egesoy, M. Basol, G. Cakan-Akdogan, Y. Akdogan, A simple desolvation method for production of cationic albumin nanoparticles with

improved drug loading and cell uptake, J. Drug Deliv. Sci. Technol. 60 (2020), 101931, https://doi.org/10.1016/j.jddst.2020.101931.
[20] E.S. Bronze-Uhle, B.C. Costa, V.F. Ximenes, P.N. Lisboa-Filho, Synthetic nanoparticles of bovine serum albumin with entrapped salicylic acid, Nanotechnol. Sci. Appl. 10 (2017) 11–21, https://doi.org/10.2147/NSA.S117018.
[21] A.N. Kovács, G. Katona, Á. Juhász, G.T. Balogh, E. Csapó, Albumin-hyaluronic acid colloidal nanocarriers: Effect of human and bovine serum albumin for intestinal ibuprofen release enhancement, J. Mol. Liq. 351 (2022), 118614, https://doi.org/10.1016/J.MOLLIQ.2022.118614.
[22] J. Reed, T.A. Reed, A set of constructed type spectra for the practical estimation of peptide secondary structure from circular dichroism, Anal. Biochem. 254 (1997) 36–40, https://doi.org/10.1006/abio.1997.2355.
[23] D. Usoltsev, V. Sitnikova, A. Kajava, M. Uspenskaya, Systematic FTIR spectroscopy study of the secondary structure changes in human serum albumin under various denaturation conditions, Biomolecules 9 (2019) 359, https://doi.org/10.3390/biom9080359.
[24] H. Abolhassani, S.A. Shojaosadati, A comparative and systematic approach to desolvation and self-assembly methods for synthesis of piperine-loaded human serum albumin nanoparticles, Colloids Surf. B Biointerfaces 184 (2019), 110534, https://doi.org/10.1016/j.colsurfb.2019.110534.
[25] P. Vidyullatha, D. Rajeswara Rao, Machine learning techniques on multidimensional curve fitting data based on r- square and chi-square methods, Int. J. Electr. Comput. Eng. 6 (2016) 974–979, https://doi.org/10.11591/ijece.v6i3.9155.
[26] Á. Juhász, D. Ungor, K. Berta, L. Seres, E. Csapó, Spreadsheet-based nonlinear analysis of in vitro release properties of a model drug from colloidal carriers, J. Mol. Liq. 328 (2021), 115405, https://doi.org/10.1016/j.molliq.2021.115405.